AD NUMBER

ADB183967

NEW LIMITATION CHANGE

TO

Approved for public release, distribution unlimited

FROM

Distribution authorized to U.S. Gov't. agencies and their contractors; Administrative/Operational Use; APR 1984. Other requests shall be referred to National Aeronautics and Space Administration, Washington, DC.

AUTHORITY

NASA TR Server Website

(1)

NASA Technical Memorandum 85793

STRESS-INTENSITY FACTOR EQUATIONS FOR CRACKS IN THREE-DIMENSIONAL FINITE BODIES SUBJECTED TO TENSION AND BENDING LOADS

J. C. Newman, Jr. and I. S. Raju

April 1984

National Aeronautics and Space Administration

Langley Research Center
Hampton, Virginia 23665

DISCLAIMER NOTICE

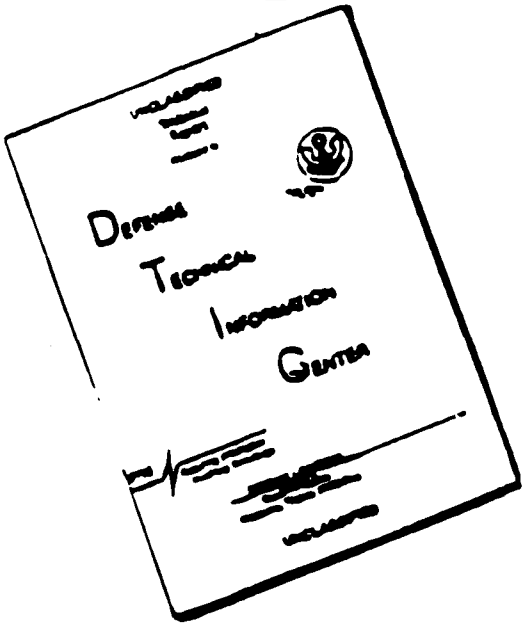

THIS DOCUMENT IS BEST QUALITY AVAILABLE. THE COPY FURNISHED TO DTIC CONTAINED A SIGNIFICANT NUMBER OF PAGES WHICH DO NOT REPRODUCE LEGIBLY.

STRESS-INTENSITY FACTOR EQUATIONS FOR CRACKS IN THREE-DIMENSIONAL FINITE BODIES SUBJECTED TO TENSION AND BENDING LOADS

J. C. Newman, Jr.[1] and I. S. Raju[2]

SUMMARY

Stress-intensity factor equations are presented for an embedded elliptical crack, a semi-elliptical surface crack, a quarter-elliptical corner crack, a semi-elliptical surface crack along the bore of a circular hole, and a quarter-elliptical corner crack at the edge of a circular hole in finite plates. The plates were subjected to either remote tension or bending loads. The stress-intensity factors used to develop these equations were obtained from previous three-dimensional finite-element analyses of these crack configurations. The equations give stress-intensity factors as a function of parametric angle, crack depth, crack length, plate thickness, and, where applicable, hole radius. The ratio of crack depth to plate thickness ranged from 0 to 1, the ratio of crack depth to crack length ranged from 0.2 to 2, and the ratio of hole radius to plate thickness ranged from 0.5 to 2. The effects of plate width on stress-intensity variations along the crack front were also included, but were either based on solutions of similar configurations or based on engineering estimates.

INTRODUCTION

In aircraft structures, fatigue failures usually occur from the initiation and propagation of cracks from notches or defects in the material that are either embedded, on the surface, or at a corner. These cracks propagate with elliptic or near-elliptic crack fronts. To predict crack-propagation life and

[1]Senior Scientist, National Aeronautics and Space Administration, Langley Research Center, Hampton, Virginia 23665
[2]Vigyan Research Associates, Hampton, Virginia

fracture strength, accurate stress-intensity factor solutions are needed for these crack configurations. But, because of the complexities of such problems, exact solutions are not available. Instead, investigators have had to use approximate analytical methods, experimental methods, or engineering estimates to obtain the stress-intensity factors.

Very few exact solutions for three-dimensional cracked bodies are available in the literature. One of these, an elliptical crack in an infinite solid subjected to uniform tension, was derived by Irwin [1] using an exact stress analysis by Green and Sneddon [2]. Kassir and Sih [3], Shah and Kobayashi [4], and Vijayakumar and Atluri [5] have obtained closed-form solutions for an elliptical crack in an infinite solid subjected to non-uniform loadings.

For finite bodies, all solutions have required approximate analytical methods. For a semi-circular surface crack in a semi-infinite solid and a semi-elliptical surface crack in a plate of finite thickness, Smith, Emery, and Kobayashi [6], and Kobayashi [7], respectively, used the alternating method to obtain stress-intensity factors along the crack front. Raju and Newman [8,9] used the finite-element method; Heliot, Labbens, and Pellissier-Tanon [10] used the boundary-integral equation method; and Nishioka and Atluri [11] used the finite-element alternating method to obtain the same information. For a quarter-elliptic corner crack in a plate, Tracey [12] and Pickard [13] used the finite-element method; Kobayashi and Enetanya [14] used the alternating method. Shah [15] estimated the stress-intensity factors for a surface crack emanating from a circular hole. For a single corner crack emanating from a circular hole in a plate, Smith and Kullgren [16] used a finite-element-alternating method to obtain the stress-intensity factors. Hechmer and Bloom [17] and Raju and Newman [18] used the finite-element method

for two symmetric corner cracks emanating from a hole in a plate. Most of these results were for limited ranges of parameters and were presented in the form of curves or tables. For ease of computation, however, results expressed in the form of equations are preferable.

The present paper presents equations for the stress-intensity factors for a wide variety of three-dimensional crack configurations subjected to either uniform remote tension or bending loads as a function of parametric angle, crack depth, crack length, plate thickness, and hole radius (where applicable); for example, see Figure 1. The equations for uniform remote tension were obtained from Reference 19. The tension equations, however, are repeated here for completeness and because the correction factors for remote bending are modifications of the tension equations. The crack configurations considered, shown in Figure 2, include: an embedded elliptical crack, a semi-elliptical surface crack, a quarter-elliptical corner crack, a semi-elliptical surface crack at a circular hole, and a quarter-elliptical corner crack at a circular hole in finite-thickness plates. The equations were based on stress-intensity factors obtained from three-dimensional finite-element analyses [8, 9, 18, and 19] that cover a wide range of configuration parameters. In some configurations, the range of the equation was extended by using stress-intensity factor solutions for a through crack in a similar configuration. In these equations, the ratio of crack depth to plate thickness (a/t) ranged from 0 to 1, the ratio of crack depth to crack length (a/c) ranged from 0.2 to 2, and the ratio of hole radius to plate thickness (r/t) ranged from 0.5 to 2. The effects of plate width (b) on stress-intensity variations along the crack front were also included, but were either based on solutions of similar configurations or based on engineering estimates.

NOMENCLATURE

a	depth of crack
b	width or half-width of cracked plate (see Fig. 2)
c	half-length of crack
F_c	boundary-correction factor for corner crack in a plate under tension
F_{ch}	boundary-correction factor for corner crack at a hole in a plate under tension
F_e	boundary-correction factor for embedded crack in a plate under tension
F_j	boundary-correction factor on stress intensity for remote tension
F_s	boundary-correction factor for surface crack in a plate under tension
F_{sh}	boundary-correction factor for surface crack at a hole in a plate under tension
f_w	finite-width correction factor
f_ϕ	angular function derived from embedded elliptical crack solution
g_i	curve fitting functions defined in text
H_c	bending multiplier for corner crack in a plate
H_{ch}	bending multiplier for corner crack at a hole in a plate
H_j	bending multiplier on stress intensity for remote bending
H_s	bending multiplier for surface crack in a plate
h	half-length of cracked plate
K	stress-intensity factor (mode I)
M	applied bending moment
M_i	curve fitting functions defined in text (i = 1, 2, or 3)
Q	shape factor for elliptical crack
r	radius of hole
S_b	remote bending stress on outer fiber, $3M/bt^2$
S_t	remote uniform tension stress
t	thickness or one-half plate thickness (see Fig. 2)

λ function defined in text

ν Poisson's ratio ($\nu = 0.3$)

ϕ parametric angle of ellipse, deg

STRESS-INTENSITY EQUATIONS

The stress-intensity factor, K, at any point along the crack front in a finite-thickness plate, such as that shown in Figure 1, was taken to be

$$K = (S_t + H_j S_b)\sqrt{\pi \frac{a}{Q}}\, F_j \tag{1a}$$

where

$$F_j = \left[M_1 + M_2\left(\frac{a}{t}\right)^2 + M_3\left(\frac{a}{t}\right)^4\right] g f_\phi f_w \tag{1b}$$

and

$$H_j = H_1 + (H_2 - H_1)\sin^p \phi \tag{1c}$$

The function Q is the shape factor for an ellipse and is given by the square of the complete elliptic integral of the second kind [2]. The boundary-correction factor, F_j, accounts for the influence of various boundaries and is a function of crack depth, crack length, hole radius (where applicable), plate thickness, plate width, and the parametric angle of the ellipse. The product $H_j F_j$ is the corresponding bending correction. The subscript j denotes the crack configuration: $j = c$ is for a corner crack in a plate, $j = e$ is for an embedded crack in a plate, $j = s$ is for a surface crack in a plate, $j = sh$ is for a surface crack at a hole in a plate, and $j = ch$ is for a corner crack at a hole in a plate. Functions M_1, M_2, M_3, H_1, H_2, and p are defined for each appropriate configuration and loading. The series containing M_1 is the boundary-correction factor at the maximum depth point. The function f_ϕ is an angular function derived from the solution for

an elliptical crack in an infinite solid. This function accounts for most of the angular variation in stress-intensity factors. The function f_w is a finite-width correction factor. Function g denotes a product of functions, such as $g_1 g_2 \cdots g_3$, that are used to fine-tune the equations. Functions H_1 and H_2 are bending multipliers obtained from bending results at ϕ equal zero and $\pi/2$, respectively. Figure 3 shows the coordinate system used to define the parametric angle, ϕ, for a/c less than and a/c greater than unity.

Very useful empirical expressions for Q have been developed by Rawe (see Ref. 9). The expressions are

$$Q = 1 + 1.464\left(\frac{a}{c}\right)^{1.65} \quad \text{for} \quad \frac{a}{c} \leq 1 \tag{2a}$$

$$Q = 1 + 1.464\left(\frac{c}{a}\right)^{1.65} \quad \text{for} \quad \frac{a}{c} > 1 \tag{2b}$$

The maximum error in the stress-intensity factor caused by using these approximate equations for Q is about 0.13 percent for all values of a/c. (Rawe's original equation was written in terms of a/2c).

In the following sections, the stress-intensity factor equations for embedded elliptical cracks, semi-elliptical surface cracks, quarter-elliptical corner cracks, semi-elliptical surface cracks at a hole, and quarter-elliptical corner cracks at a hole in finite plates (see Fig. 2) subjected to either remote tension or bending loads are presented. The particular functions chosen were obtained from curve fitting to finite-element results [8, 9, 18, and 19] by using polynomials in terms of a/c, a/t, and angular functions of ϕ. For cracks emanating from holes, polynomial equations in terms of c/r and ϕ were also used. Typical results will be presented for

$a/c = 0.2$, 0.5, 1, and 2 with a/t varying from 0 to 1. Table 1 gives the range of applicability of ϕ, a/t, a/c, r/t, and $(r + c)/b$ for the proposed equations.

Embedded Elliptical Crack

The stress-intensity factor equation for an embedded elliptical crack in a finite plate, Figure 2(a), subjected to tension was obtained by fitting equation (1) to finite-element results in Reference 19. The results of Irwin [1] were used to account for the limiting behavior as a/c approaches zero or infinity. The equation is

$$K = S_t \sqrt{\pi \frac{a}{Q}}\, F_e\left(\frac{a}{c}, \frac{a}{t}, \frac{c}{b}, \phi\right) \tag{3}$$

for $0 < a/c < \infty$, $c/b < 0.5$, and $-\pi < \phi < \pi$ provided that a/t satisfies:

$$\left.\begin{aligned} &\frac{a}{t} < 1.25\left(\frac{a}{c} + 0.6\right) \quad \text{for} \quad 0 < \frac{a}{c} < 0.2 \\ &\frac{a}{t} < 1 \qquad\qquad\qquad \text{for} \quad 0.2 < \frac{a}{c} < \infty \end{aligned}\right\} \tag{4}$$

The function F_e accounts for the influence of crack shape (a/c), crack size (a/t), finite width (c/b), and angular location (ϕ), and was chosen as

$$F_e = \left[M_1 + M_2\left(\frac{a}{t}\right)^2 + M_3\left(\frac{a}{t}\right)^4\right] g\, f_\phi\, f_w \tag{5}$$

The term in brackets gives the boundary-correction factors at $\phi = \pi/2$ (where $g = f_\phi = 1$). The function f_ϕ was taken from the exact solution for an embedded elliptical crack in an infinite solid [1] and f_w is a finite-width correction factor. The function g is a fine-tuning curve-fitting function.

For $a/c < 1$:

$$M_1 = 1 \tag{6}$$

$$M_2 = \frac{0.05}{0.11 + \left(\frac{a}{c}\right)^{3/2}} \tag{7}$$

$$M_3 = \frac{0.29}{0.23 + \left(\frac{a}{c}\right)^{3/2}} \tag{8}$$

$$g = 1 - \frac{\left(\frac{a}{t}\right)^4 \left(2.6 - 2\,\frac{a}{t}\right)^{1/2}}{1 + 4\left(\frac{a}{c}\right)} \left|\cos \phi\right| \tag{9}$$

and

$$f_\phi = \left[\left(\frac{a}{c}\right)^2 \cos^2 \phi + \sin^2 \phi\right]^{1/4} \tag{10}$$

(Note that eq. (9) is slightly different, and is believed to be more accurate, than that given in Ref. 19.) The finite-width correction, f_w, from Reference 9 was

$$f_w = \left[\sec\left(\frac{\pi c}{2b}\sqrt{\frac{a}{t}}\right)\right]^{1/2} \tag{11}$$

for $c/b < 0.5$. (Note that for the embedded crack, t is defined as one-half of the full plate thickness.)

For $a/c > 1$:

$$M_1 = \sqrt{\frac{c}{a}} \tag{12}$$

and

$$f_\phi = \left[\left(\frac{c}{a}\right)^2 \sin^2\phi + \cos^2\phi\right]^{1/4} \tag{13}$$

The functions M_2, M_3, g, and f_w are the same as equations (7), (8), (9), and (11), respectively.

Figure 4 shows some typical boundary-correction factors for various crack shapes (a/c = 0.2, 0.5, 1, and 2) with a/t equal to 0, 0.5, 0.75, and 1. The correction factor, F_e, is plotted against the parameter angle, ϕ. At $\phi = 0$, the point on the crack front that is located at the center of the plate, the influence of plate thickness is much less than at $\phi = \pi/2$, the point that is located closest to the plate surface. The results shown for a/t = 0 are the exact solutions for an elliptical crack in an infinite solid [1]. For a/t < 0.8, the results from the equation are within about 3 percent of the finite-element results. (Herein, "percent" error is defined as the difference between the equation and the finite-element results normalized by the maximum value for that particular case. This definition is necessary because, in some cases, the stress-intensity factor ranges from positive to negative along the crack front.) For a/t > 0.8, the accuracy of equation (3) has not been established. But its use in that range appears to be supported by estimates based on an embedded crack approaching a through crack (see Ref. 19).

Bending equations were not developed for the embedded elliptical crack.

Semi-Elliptical Surface Crack

The equations for the stress-intensity factors for a semi-elliptical surface crack in a finite plate, Figure 2(b), subjected to remote tension and bending loads were obtained from Reference 9. The tension and bending

equations were previously fitted to finite-element results from Raju and Newman [8] for a/c values less than or equal to unity. Equations for tension and bending loads for a/c greater than unity were developed herein. The results of Gross and Srawley [20] for a single-edge crack were used to account for the limiting behavior as a/c aproaches zero. The equation is

$$K = (S_t + H_s S_b)\sqrt{\pi \frac{a}{Q}}\, F_s\left(\frac{a}{c}, \frac{a}{t}, \frac{c}{b}, \phi\right) \tag{14}$$

for $0 < a/c < 2$, $c/b < 0.5$, and $0 < \phi < \pi$, again, provided that a/t satisfies equation (4). The function F_s was chosen to be

$$F_s = \left[M_1 + M_2\left(\frac{a}{t}\right)^2 + M_3\left(\frac{a}{t}\right)^4\right] g\, f_\phi\, f_w \tag{15}$$

For $a/c < 1$:

$$M_1 = 1.13 - 0.09\left(\frac{a}{c}\right) \tag{16}$$

$$M_2 = -0.54 + \frac{0.89}{0.2 + \frac{a}{c}} \tag{17}$$

$$M_3 = 0.5 - \frac{1}{0.65 + \frac{a}{c}} + 14\left(1 - \frac{a}{c}\right)^{24} \tag{18}$$

$$g = 1 + \left[0.1 + 0.35\left(\frac{a}{t}\right)^2\right](1 - \sin\phi)^2 \tag{19}$$

and f_ϕ is given by equation (10). The finite-width correction, f_w, is again given by equation (11). Equations (15) through (19) were taken from Reference 9. (The large power in eq. (18) was needed to fit the behavior as a/c approaches zero.)

The bending multiplier, H_j, in equation (1) has the form

$$H_j = H_1 + (H_2 - H_1) \sin^p \phi \tag{20}$$

where H_1, H_2, and p are defined for each crack configuration considered. For the surface crack ($j = s$),

$$p = 0.2 + \frac{a}{c} + 0.6\,\frac{a}{t} \tag{21}$$

$$H_1 = 1 - 0.34\,\frac{a}{t} - 0.11\,\frac{a}{c}\left(\frac{a}{t}\right) \tag{22}$$

and

$$H_2 = 1 + G_{21}\left(\frac{a}{t}\right) + G_{22}\left(\frac{a}{t}\right)^2 \tag{23}$$

In this equation for H_2,

$$G_{21} = -1.22 - 0.12\,\frac{a}{c} \tag{24}$$

$$G_{22} = 0.55 - 1.05\left(\frac{a}{c}\right)^{0.75} + 0.47\left(\frac{a}{c}\right)^{1.5} \tag{25}$$

Equations (21) through (25) were taken from Reference 9.

<u>For $a/c > 1$:</u>

$$M_1 = \sqrt{\frac{c}{a}}\left(1 + 0.04\,\frac{c}{a}\right) \tag{26}$$

$$M_2 = 0.2\left(\frac{c}{a}\right)^4 \tag{27}$$

$$M_3 = -0.11\left(\frac{c}{a}\right)^4 \tag{28}$$

$$g = 1 + \left[0.1 + 0.35\left(\frac{c}{a}\right)\left(\frac{a}{t}\right)^2\right](1 - \sin\phi)^2 \tag{29}$$

and f_ϕ and f_w are given by equations (13) and (11), respectively.

The bending multiplier for $a/c > 1$ is also given by equation (20) where

$$p = 0.2 + \frac{c}{a} + 0.6\,\frac{a}{t} \tag{30}$$

$$H_1 = 1 + G_{11}\,\frac{a}{t} + G_{12}\left(\frac{a}{t}\right)^2 \tag{31}$$

$$H_2 = 1 + G_{21}\,\frac{a}{t} + G_{22}\left(\frac{a}{t}\right)^2 \tag{32}$$

$$G_{11} = -0.04 - 0.41\,\frac{c}{a} \tag{33}$$

$$G_{12} = 0.55 - 1.93\left(\frac{c}{a}\right)^{0.75} + 1.38\left(\frac{c}{a}\right)^{1.5} \tag{34}$$

$$G_{21} = -2.11 + 0.77\,\frac{c}{a} \tag{35}$$

and

$$G_{22} = 0.55 - 0.72\left(\frac{c}{a}\right)^{0.75} + 0.14\left(\frac{c}{a}\right)^{1.5} \tag{36}$$

Figures 5 and 6 show some typical boundary-correction factors for various surface crack shapes ($a/c = 0.2$, 0.5, 1, and 2) with a/t equal to 0, 0.5, and 1 for tension and bending, respectively. For all combinations of parameters investigated and $a/t \leq 0.8$, equation (14) was within ±5 percent of the finite-element results ($0.2 \leq a/c \leq 2$) and the single-edge crack solution ($a/c = 0$). For $a/t > 0.8$, the accuracy of equation (14) has not been established. However, its use in that range appears to be supported by estimates based on a surface crack approaching a through crack.

The use of negative stress-intensity factors in the case of bending are applicable only when there is sufficient tension to keep the crack surfaces open; that is, the total stress-intensity factor due to combined tension and bending must be positive.

Quarter-Elliptical Corner Crack

The stress-intensity factor equations for a quarter-elliptical corner crack in a finite plate, Figure 2(c), subjected to tension and bending loads were obtained by fitting equation (1) to the finite-element results in Reference 19 for tension and the results in Table 1 for bending. The equation is

$$K = (S_t + H_c S_b)\sqrt{\pi \frac{a}{Q}}\, F_c\left(\frac{a}{c}, \frac{a}{t}, \frac{c}{b}, \phi\right) \tag{37}$$

for $0.2 \leq a/c \leq 2$, $a/t < 1$, and $0 \leq \phi \leq \pi/2$ for $\frac{c}{b} < 0.5$. The function F_c was chosen as

$$F_c = \left[M_1 + M_2\left(\frac{a}{t}\right)^2 + M_3\left(\frac{a}{t}\right)^4\right] g_1\, g_2\, f_\phi\, f_w \tag{38}$$

For $a/c \leq 1$:

$$M_1 = 1.08 - 0.03\left(\frac{a}{c}\right) \tag{39}$$

$$M_2 = -0.44 + \frac{1.06}{0.3 + \frac{a}{c}} \tag{40}$$

$$M_3 = -0.5 + 0.25\left(\frac{a}{c}\right) + 14.8\left(1 - \frac{a}{c}\right)^{15} \tag{41}$$

$$g_1 = 1 + \left[0.08 + 0.4\left(\frac{a}{t}\right)^2\right](1 - \sin\phi)^3 \tag{42}$$

$$g_2 = 1 + \left[0.08 + 0.15\left(\frac{a}{t}\right)^2\right](1 - \cos\phi)^3 \qquad (43)$$

and f_ϕ is given by equation (10). The finite-width correction, f_w, was estimated herein by using the single-edge crack tension solution given in Reference 21 (divided by 1.12) and was

$$f_w = 1 - 0.2\lambda + 9.4\lambda^2 - 19.4\lambda^3 + 27.1\lambda^4 \qquad (44)$$

where $\lambda = \frac{c}{b}\sqrt{\frac{a}{t}}$. (The width correction from Ref. 21 was divided by 1.12 because the front-face correction was already included in eq. (38).) Equation (44) is restricted to $c/b < 0.5$.

As a/t approaches unity, with $a/c = 1$ and $\phi = 0$, the stress-intensity factor equation (eq. (37)) for tension reduces to

$$K = S_t\sqrt{\pi c}\ 1.11 f_w \qquad (45)$$

Equation (45) is within about 1 percent of the accepted solution [21] for $c/b < 0.6$.

The bending multiplier, H_c, has the form given by equation (20). Functions p, H_1, H_2, and G_{21} are given by equations (21)-(24), respectively, for $a/c < 1$. The function G_{22} is

$$G_{22} = 0.64 - 1.05\left(\frac{a}{c}\right)^{0.75} + 0.47\left(\frac{a}{c}\right)^{1.5} \qquad (46)$$

For $a/c > 1$:

$$M_1 = \sqrt{\frac{c}{a}}\left(1.08 - 0.03\,\frac{c}{a}\right) \qquad (47)$$

$$M_2 = 0.375\left(\frac{c}{a}\right)^2 \qquad (48)$$

$$M_3 = -0.25\left(\frac{c}{a}\right)^2 \tag{49}$$

$$g_1 = 1 + \left[0.08 + 0.4\left(\frac{c}{t}\right)^2\right](1 - \sin\phi)^3 \tag{50}$$

$$g_2 = 1 + \left[0.08 + 0.15\left(\frac{c}{t}\right)^2\right](1 - \cos\phi)^3 \tag{51}$$

and f_ϕ is given by equation (13). The finite-width correction is, again, given by equation (44).

The bending-correction factor H_c is, again, given by equation (20) where p, H_1, H_2, G_{11}, G_{12}, and G_{21} are given by equations (30)-(35), respectively. The function G_{22} is given by

$$G_{22} = 0.64 - 0.72\left(\frac{c}{a}\right)^{0.75} + 0.14\left(\frac{c}{a}\right)^{1.5} \tag{52}$$

Figures 7 and 8 show some typical boundary-correction factors for corner cracks in plates for various crack shapes (a/c = 0.2, 0.5, 1, and 2) with a/t varying from 0 to 1 for tension and bending, respectively. At a/t = 0, the results for tension and bending are identical. As expected, for tension the effects of a/t are much larger at lower values of a/c. Again, the use of negative stress-intensity factors in this case of bending are applicable only when there is sufficient tension to keep the crack surfaces open (stress-intensity factor due to combined tension and bending must be positive).

Semi-Elliptical Surface Crack at Hole

Two symmetric surface cracks.- The stress-intensity factor equation for two symmetric semi-elliptical surface cracks located along the bore of a hole in a finite plate, Figure 2(d), subjected to tension was obtained by fitting equation (1) to finite-element results [19]. The equation is

$$K = S_t \sqrt{\pi \frac{a}{Q}}\, F_{sh}\left(\frac{a}{c}, \frac{a}{t}, \frac{r}{t}, \frac{r}{b}, \frac{c}{b}, \phi\right) \tag{53}$$

for $0.2 \leq a/c \leq 2$, $a/t \leq 1$, $0.5 \leq r/t \leq 2$, $(r + c)/b \leq 0.5$, and $-\pi/2 \leq \phi \leq \pi/2$. (Note that here t is defined as one-half of the full plate thickness.) The function F_{sh} was chosen as

$$F_{sh} = \left[M_1 + M_2\left(\frac{a}{t}\right)^2 + M_3\left(\frac{a}{t}\right)^4\right] g_1\, g_2\, g_3\, f_\phi\, f_w \tag{54}$$

For $a/c \leq 1$:

$$M_1 = 1 \tag{55}$$

$$M_2 = \frac{0.05}{0.11 + \left(\frac{a}{c}\right)^{3/2}} \tag{56}$$

$$M_3 = \frac{0.29}{0.23 + \left(\frac{a}{c}\right)^{3/2}} \tag{57}$$

$$g_1 = 1 - \frac{\left(\frac{a}{t}\right)^4 \left(2.6 - 2\,\frac{a}{t}\right)^{1/2}}{1 + 4\left(\frac{a}{c}\right)} \cos\phi \tag{58}$$

$$g_2 = \frac{1 + 0.358\lambda + 1.425\lambda^2 - 1.578\lambda^3 + 2.156\lambda^4}{1 + 0.08\lambda^2} \tag{59}$$

$$\lambda = \frac{1}{1 + \frac{c}{r}\cos(0.9\phi)} \tag{60}$$

$$g_3 = 1 + 0.1(1 - \cos\phi)^2\left(1 - \frac{a}{t}\right)^{10} \tag{61}$$

(Note that eq. (58) is slightly different, and is believed to be more accurate, than that given in Ref. 19.) The function f_ϕ is given by equation (10).

The finite-width correction, f_w, was taken as

$$f_w = \left\{ \sec\left(\frac{\pi r}{2b}\right) \sec\left[\frac{\pi(2r + nc)}{4(b - c) + 2nc} \sqrt{\frac{a}{t}} \right] \right\}^{1/2} \tag{62}$$

where $n = 1$ is for a single crack and $n = 2$ is for two-symmetric cracks. This equation was chosen to account for the effects of width on stress concentration at the hole [22] and for crack eccentricity [21]. For $a/c > 1$:

$$M_1 = \sqrt{\frac{c}{a}} \tag{63}$$

The functions M_2, M_3, g_1, g_2, g_3, and λ are given by equations (56) through (61), and the functions f_ϕ and f_w are given by equations (13) and (62), respectively.

Estimates for a single-surface crack.- The stress-intensity factors for a single-surface crack located along the bore of a hole were estimated from the present results for two symmetric surface cracks by using a conversion factor developed by Shah [15]. The relationship between one- and two-surface cracks was given by

$$(K)_{\substack{\text{one} \\ \text{crack}}} = \sqrt{\frac{\frac{4}{\pi} + \frac{ac}{2tr}}{\frac{4}{\pi} + \frac{ac}{tr}}} \, (K)_{\substack{\text{two} \\ \text{cracks}}} \tag{64}$$

where K for two cracks must be evaluated for an infinite plate ($f_w = 1$) and then the finite-width correction for one crack must be applied. Shah had assumed that the conversion factor was constant for all locations along the crack front, that is, independent of the parametric angle.

Figure 9 shows some typical boundary-correction factors for a single surface crack at a hole for various crack shapes ($a/c = 0.2$, 0.5, 1, and 2) with a/t varying from 0 to 1. These results were in good agreement with

boundary-correction factors estimated by Shah [15]. The agreement was generally within about 2 percent except where the crack intersects the free surface ($2\phi/\pi = 1$). Here the equation gave results that were 2 to 5 percent higher than those estimated by Shah.

Stress-intensity factor equations for bending were not developed for a surface crack located at the center of a hole.

Quarter-Elliptical Corner Crack at a Hole

Two symmetric corner cracks.- The stress-intensity factor equations for two symmetric quarter-elliptical corner cracks at a hole in a finite plate, Figure 2(e), subjected to remote tension and bending loads were obtained by fitting to finite-element results in Reference 18. The equation is

$$K = (S_t + H_{ch} S_b) \sqrt{\pi \frac{a}{Q}}\, F_{ch}\left(\frac{a}{c}, \frac{a}{t}, \frac{r}{t}, \frac{r}{b}, \frac{c}{b}, \phi\right) \tag{65}$$

for $0.2 \le a/c \le 2$, $a/t \le 1$, $0.5 \le r/t \le 2$, $(r + c)/b \le 0.5$, and $0 \le \phi \le \pi/2$. The function F_{ch} was chosen as

$$F_{ch} = \left[M_1 + M_2\left(\frac{a}{t}\right)^2 + M_3\left(\frac{a}{t}\right)^4\right] g_1\, g_2\, g_3\, g_4\, f_\phi\, f_w \tag{66}$$

For $a/c \le 1$:

$$M_1 = 1.13 - 0.09\left(\frac{a}{c}\right) \tag{67}$$

$$M_2 = -0.54 + \frac{0.89}{0.2 + \frac{a}{c}} \tag{68}$$

$$M_3 = 0.5 - \frac{1}{0.65 + \frac{a}{c}} + 14\left(1 - \frac{a}{c}\right)^{24} \tag{69}$$

$$g_1 = 1 + \left[0.1 + 0.35\left(\frac{a}{t}\right)^2\right](1 - \sin\phi)^2 \tag{70}$$

$$g_2 = \frac{1 + 0.358\lambda + 1.425\lambda^2 - 1.578\lambda^3 + 2.156\lambda^4}{1 + 0.13\lambda^2} \tag{71}$$

where

$$\lambda = \frac{1}{1 + \frac{c}{r}\cos(\mu\phi)} \tag{72}$$

$\mu = 0.85$ for tension and $\mu = 0.85 - 0.25(a/t)^{1/4}$ for bending. The functions g_3 and g_4 are given by

$$g_3 = \left(1 + 0.04\,\frac{a}{c}\right)\left[1 + 0.1(1 - \cos\phi)^2\right]\left[0.85 + 0.15\left(\frac{a}{t}\right)^{1/4}\right] \tag{73}$$

and

$$g_4 = 1 - 0.7\left(1 - \frac{a}{t}\right)\left(\frac{a}{c} - 0.2\right)\left(1 - \frac{a}{c}\right) \tag{74}$$

Functions f_ϕ and f_w are given by equations (10) and (62), respectively.

The bending multiplier, H_{ch}, is given by equation (2C) for $a/c < 1$. The terms p, H_1, and H_2 are given by

$$p = 0.1 + 1.3\,\frac{a}{t} + 1.1\,\frac{a}{c} - 0.7\,\frac{a}{c}\left(\frac{a}{t}\right) \tag{75}$$

$$H_1 = 1 + G_{11}\,\frac{a}{t} + G_{12}\left(\frac{a}{t}\right)^2 + G_{13}\left(\frac{a}{t}\right)^3 \tag{76}$$

and

$$H_2 = 1 + G_{21}\,\frac{a}{t} + G_{22}\left(\frac{a}{t}\right)^2 + G_{23}\left(\frac{a}{t}\right)^3 \tag{77}$$

where

$$G_{11} = -0.43 - 0.74\,\frac{a}{c} - 0.84\left(\frac{a}{c}\right)^2 \tag{78}$$

$$G_{12} = 1.25 - 1.19\,\frac{a}{c} + 4.39\left(\frac{a}{c}\right)^2 \tag{79}$$

$$G_{13} = -1.94 + 4.22\,\frac{a}{c} - 5.51\left(\frac{a}{c}\right)^2 \tag{80}$$

$$G_{21} = -1.5 - 0.04\,\frac{a}{c} - 1.73\left(\frac{a}{c}\right)^2 \tag{81}$$

$$G_{22} = 1.71 - 3.17\,\frac{a}{c} + 6.84\left(\frac{a}{c}\right)^2 \tag{82}$$

$$G_{23} = -1.28 + 2.71\,\frac{a}{c} - 5.22\left(\frac{a}{c}\right)^2 \tag{83}$$

For $a/c > 1$:

$$M_1 = \sqrt{\frac{c}{a}}\left(1 + 0.04\,\frac{c}{a}\right) \tag{84}$$

$$M_2 = 0.2\left(\frac{c}{a}\right)^4 \tag{85}$$

$$M_3 = -0.11\left(\frac{c}{a}\right)^4 \tag{86}$$

$$g_1 = 1 + \left[0.1 + 0.35\left(\frac{c}{a}\right)\left(\frac{a}{t}\right)^2\right](1 - \sin\phi)^2 \tag{87}$$

Functions g_2 and λ are given by equations (71) and (72). Function g_3 is given by

$$g_3 = 1.13 - 0.09\,\frac{c}{a}\left[1 + 0.1(1 - \cos\phi)^2\right]\left[0.85 + 0.15\left(\frac{a}{t}\right)^{1/4}\right] \tag{88}$$

and $g_4 = 1$. The functions f_ϕ and f_w are, again, given by equations (13) and (62), respectively.

Again, the bending-correction factor, H_{ch}, is given by equation (20). The function ρ is given by equation (30) for $a/c > 1$. The H-functions are given by equations (75) and (76) where

$$G_{11} = -2.07 + 0.06 \frac{c}{a} \tag{89}$$

$$G_{12} = 4.35 + 0.16 \frac{c}{a} \tag{90}$$

$$G_{13} = -2.93 - 0.3 \frac{c}{a} \tag{91}$$

$$G_{21} = -3.64 + 0.37 \frac{c}{a} \tag{92}$$

$$G_{22} = 5.87 - 0.49 \frac{c}{a} \tag{93}$$

$$G_{23} = -4.32 + 0.53 \frac{c}{a} \tag{94}$$

Estimates for a single-corner crack.- The stress-intensity factors for a single-corner crack at a hole were estimated from the present results for two-symmetric corner cracks by using the Shah-conversion factor (eq. (64)). Raju and Newman [18] have evaluated the use of the conversion factor for some corner-crack-at-a-hole configurations. The stress-intensity factor obtained using the conversion factor were in good agreement with the results from Smith and Kullgren [16] for a single-corner crack at a hole.

Figures 10 and 11 show some typical boundary-correction factors for a single corner crack at a hole for various a/c and a/t ratios for tension and bending, respectively. Again, the use of negative stress-intensity factors in the case of bending are applicable only when there is sufficient tension to make the total stress-intensity factor, due to combined tension and bending, positive.

CONCLUDING REMARKS

Stress-intensity factors from three-dimensional finite-element analyses were used to develop stress-intensity factor equations for a wide variety of crack configurations subjected to either remote uniform tension or bending loads. The following configurations were included: an embedded elliptical crack, a semi-elliptical surface crack, a quarter-elliptical corner crack, a semi-elliptical surface crack along the bore of a hole, and a quarter-elliptical corner crack at the edge of a hole in finite plates. The equations cover a wide range of configuration parameters. The ratio of crack depth to plate thickness (a/t) ranged from 0 to 1, the ratio of crack depth to crack length (a/c) ranged from 0.2 to 2, and the ratio of hole radius to plate thickness (r/t) ranged from 0.5 to 2 (where applicable). The effects of plate width (b) on stress-intensity variations along the crack front were also included, but were based on engineering estimates.

For all configurations for which ratios of crack depth to plate thickness do not exceed 0.8, the equations are generally within 5 percent of the finite-element results, except where the crack front intersects a free surface. Here the proposed equations give higher stress-intensity factors than the finite-element results, but these higher values probably represent the limiting behavior as the mesh is refined near the free surface. For ratios greater than 0.8, no solutions are available for direct comparison; however, the equations appear reasonable on the basis of engineering estimates.

The stress-intensity factor equations presented herein should be useful for correlating and predicting fatigue-crack-growth rates as well as in computing fracture toughness and fracture loads for these types of crack configurations.

REFERENCES

[1] Irwin, G. R.: The Crack Extension Force for a Part-Through Crack in a Plate, ASME, J. Appl. Mechs., Vol. 29, No. 4, 1962, pp. 651-654.

[2] Green, A. E.; and Sneddon, I. N.: The Distribution of Stress in the Neighborhood of a Flat Elliptical Crack in an Elastic Solid, Proc. Cambridge Phil. Soc., Vol. 47, 1950, pp. 159-164.

[3] Kassir, M. K.; and Sih, G. C.: Three-Dimensional Stress Distribution Around an Elliptical Crack Under Arbitrary Loadings, Journal of Applied Mechanics, Vol. 88, 1966, pp. 601-611.

[4] Shah, R. C.; and Kobayashi, A. S.: Stress-Intensity Factor for an Elliptical Crack Under Arbitrary Normal Loading, Engineering Fracture Mechanics, Vol. 3, 1971, pp. 71-96.

[5] Vijayakumar, K.; and Atluri, S. N.: An Embedded Elliptical Flaw in an Infinite Solid, Subject to Arbitrary Crack-Face Tractions, Journal of Applied Mechanics, Vol. 48, 1981, pp. 88-96.

[6] Smith, F. W.; Emery, A. F.; and Kobayashi, A. S.: Stress Intensity Factors for Semi-Circular Cracks, Part 2 - Semi-Infinite Solid, J. Appl. Mechs., Vol. 34, No. 4, Trans. ASME, Vol. 89, Series E, Dec. 1967, pp. 953-959.

[7] Kobayashi, A. S.: Crack-Opening Displacement in a Surface Flawed Plate Subjected to Tension or Plate Bending, Proc. Second Int. Conf. on Mechanical Behavior of Materials, ASM, 1976, pp. 1073-1077.

[8] Raju, I. S.; and Newman, J. C., Jr.: Stress-Intensity Factors for a Wide Range of Semi-Elliptical Surface Cracks in Finite-Thickness Plates, Engineering Fracture Mechanics J., Vol. 11, No. 4, 1979, pp. 817-829.

[9] Newman, J. C., Jr.; and Raju, I. S.: Analyses of Surface Cracks in Finite Plates Under Tension or Bending Loads, NASA TP-1578, Dec. 1979.

[10] Heliot, J.; Labbens, R.; and Pellissier-Tanon, A.: Benchmark Problem No. 1 - Semi-Elliptical Surface Crack, Int. J. of Fracture, Vol. 15, No. 6, Dec. 1979, pp. R197-R202.

[11] Nishioka, T.; and Atluri, S. N.: Analytical Solution for Embedded Elliptical Cracks, and Finite Element-Alternating Method for Elliptical Surface Cracks, Subjected to Arbitrary Loadings, Engineering Fracture Mechanics, Vol. 17, 1983, pp. 247-268.

[12] Tracey, D. M.: 3D Elastic Singularity Element for Evaluation of K Along an Arbitrary Crack Front, Int. J. of Fracture, Vol. 9, 1973, pp. 340-343.

[13] Pickard, A. C.: Stress Intensity Factors for Cracks with Circular and Elliptic Crack Fronts-Determined by 3D Finite Element Methods, PNR-90035, Rolls-Royce Limited, May 1980.

[14] Kobayashi, A. S.; and Smetanya, A. N.: Stress Intensity Factor of a Corner Crack, Mechanics of Crack Growth, ASTM STP-590, American Society for Testing and Materials, 1976, pp. 477-495.

[15] Shah, R. C.: Stress Intensity Factors for Through and Part-Through Cracks Originating at Fastener Holes, Mechanics of Crack Growth, ASTM STP-590, American Society for Testing and Materials, 1976, pp. 429-459.

[16] Smith, F. W.; and Kullgren, T. E.: Theoretical and Experimental Analysis of Surface Cracks Emanating from Fastener Holes, AFFDL-TR-76-104, Air Force Flight Dynamics Laboratory, Feb. 1977.

[17] Heckner, J. L.; and Bloom, J. M.: Determination of Stress Intensity Factors for the Corner-Cracked Hole Using the Isoparametric Singularity Element, Int. J. of Fracture, Oct. 1977.

[18] Raju, I. S.; and Newman, J. C., Jr.: Stress-Intensity Factors for Two Symmetric Corner Cracks, Fracture Mechanics, ASTM STP-677, C. W. Smith, Ed., American Society of Testing and Materials, 1979, pp. 411-430.

[19] Newman, J. C., Jr.; and Raju, I. S.: Stress-Intensity Factor Equations for Cracks in Three-Dimensional Finite Bodies, Fracture Mechanics - Volume I: Theory and Analysis, ASTM STP-791, J. C. Lewis and G. Sines, Eds., American Society of Testing and Materials, 1983, pp. I-238, I-265.

[20] Gross, B.; and Srawley, J. E.: Stress-Intensity Factors for Single-Edge-Notch Specimens in Bending or Combined Bending and Tension by Boundary Collocation of a Stress function, NASA TN D-2603, 1965.

[21] Tada, H.; Paris, P. C.; and Irwin, G. R.: The Stress Analysis of Cracks Handbook, Del Research Corporation, 1973.

[22] Howland, R. C. J.: On the Stresses in the Neighbourhood of a Circular Hole in a Strip Under Tension, Philos. Trans. R. Soc. London, Series A, Vol. 229, Jan. 1930, pp. 49-86.

Table 1. Range of applicability for stress-intensity factor equations.

Configuration	Equation	ϕ	a/t	a/c	r/t	(r + c)/b
Embedded Crack in Plate[a]	(3)	$-\pi$ to π	(b)	0 to ∞	...	<0.5[c]
Surface Crack in Plate	(14)	0 to π	(b)	0 to 2	...	<0.5[c]
Corner Crack in Plate	(37)	0 to $\frac{\pi}{2}$	<1	0.2 to 2	...	<0.5[c]
Surface Crack at Hole[a,d]	(53)	$-\frac{\pi}{2}$ to $\frac{\pi}{2}$	<1	0.2 to 2	0.5 to 2	<0.5
Corner Crack at Hole[d]	(65)	0 to $\frac{\pi}{2}$	(e)	0.2 to 2	0.5 to 2	<0.5

[a] Equations for bending were not developed for this case.

[b] $a/t < 1.25\ (a/c + 0.6)$ for $0 \leq a/c \leq 0.2$ and $a/t < 1$ for $a/c > 0.2$.

[c] $r = 0$.

[d] One or two-symmetric cracks.

[e] $a/t < 1$ for remote tension and $a/t \leq 0.8$ for remote bending.

Table 2. Boundary-correction factors, F_cH_c, for quarter-elliptical corner crack in a plate subjected to bending $\left(\nu = 0.3;\ F_cH_c = K/\left(S_b\sqrt{\pi a/Q}\ \right)\right)$.

		a/t		
a/c	$2\phi/\pi$	0.2	0.5	0.8
	0	0.522	0.609	0.779
	0.25	0.669	0.702	0.808
0.2	0.5	0.801	0.746	0.716
	0.75	0.868	0.746	0.577
	1.0	0.876	0.750	0.604
	0	0.740	0.799	0.904
	0.25	0.724	0.690	0.670
0.4	0.5	0.785	0.632	0.451
	0.75	0.826	0.583	0.272
	1.0	0.846	0.569	0.262
	0	1.084	1.046	1.027
	0.25	0.934	0.770	0.604
1.0	0.5	0.838	0.547	0.237
	0.75	0.798	0.417	0.011
	1.0	0.839	0.407	-0.032
	0	0.932	0.811	0.734
	0.25	0.851	0.623	0.442
2.0	0.5	0.761	0.413	0.105
	0.75	0.700	0.268	-0.131
	1.0	0.677	0.215	-0.206

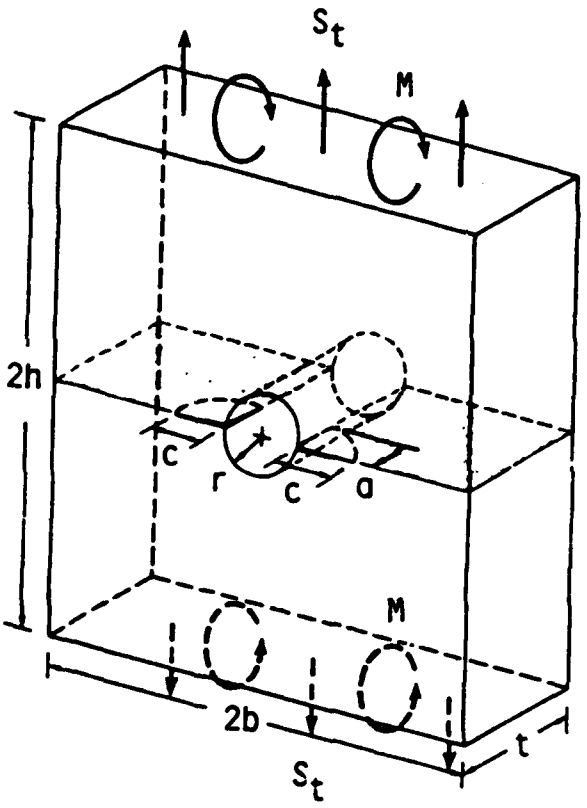

$$S_b = \frac{3M}{bt^2}$$

Fig. 1--Corner cracks at the edge of a hole in a finite plate subjected to remote tension and bending.

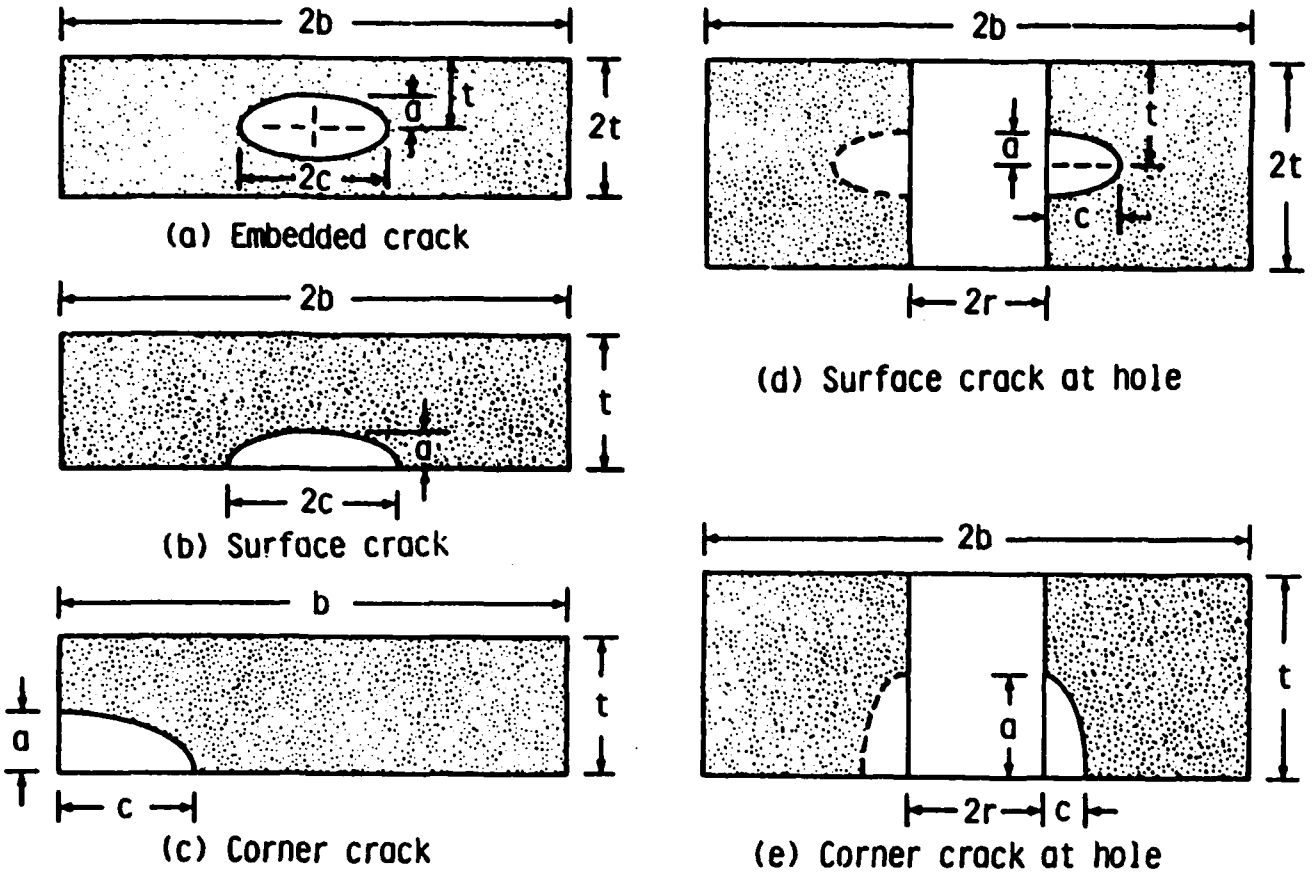

Fig. 2--Embedded-, surface-, and corner-crack configurations (all cracks have elliptical fronts).

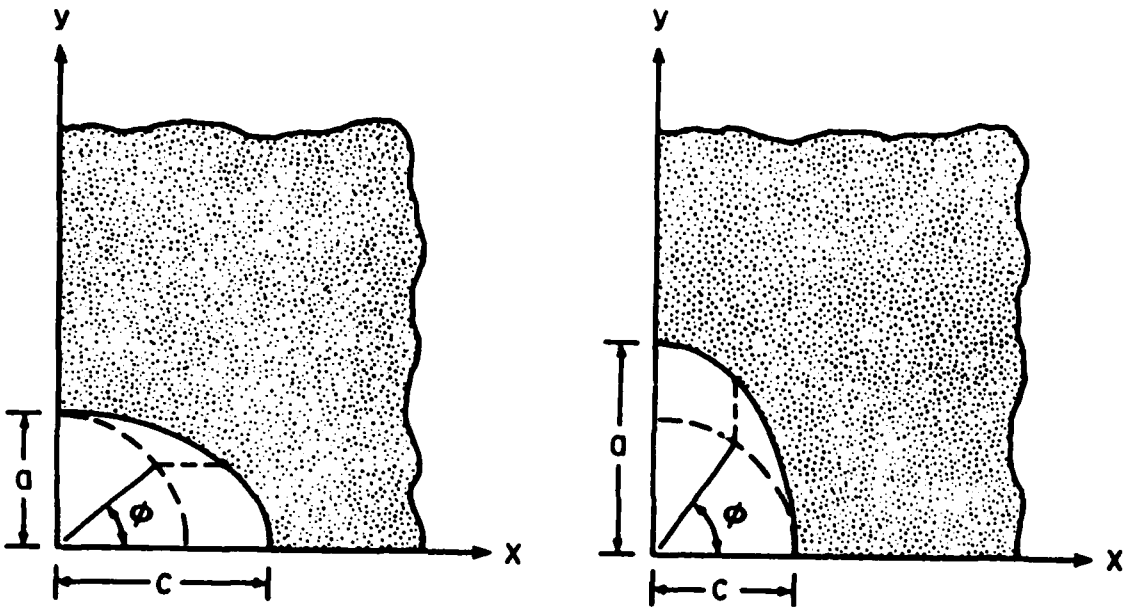

Fig. 3--Coordinate system used to define parametric angle.

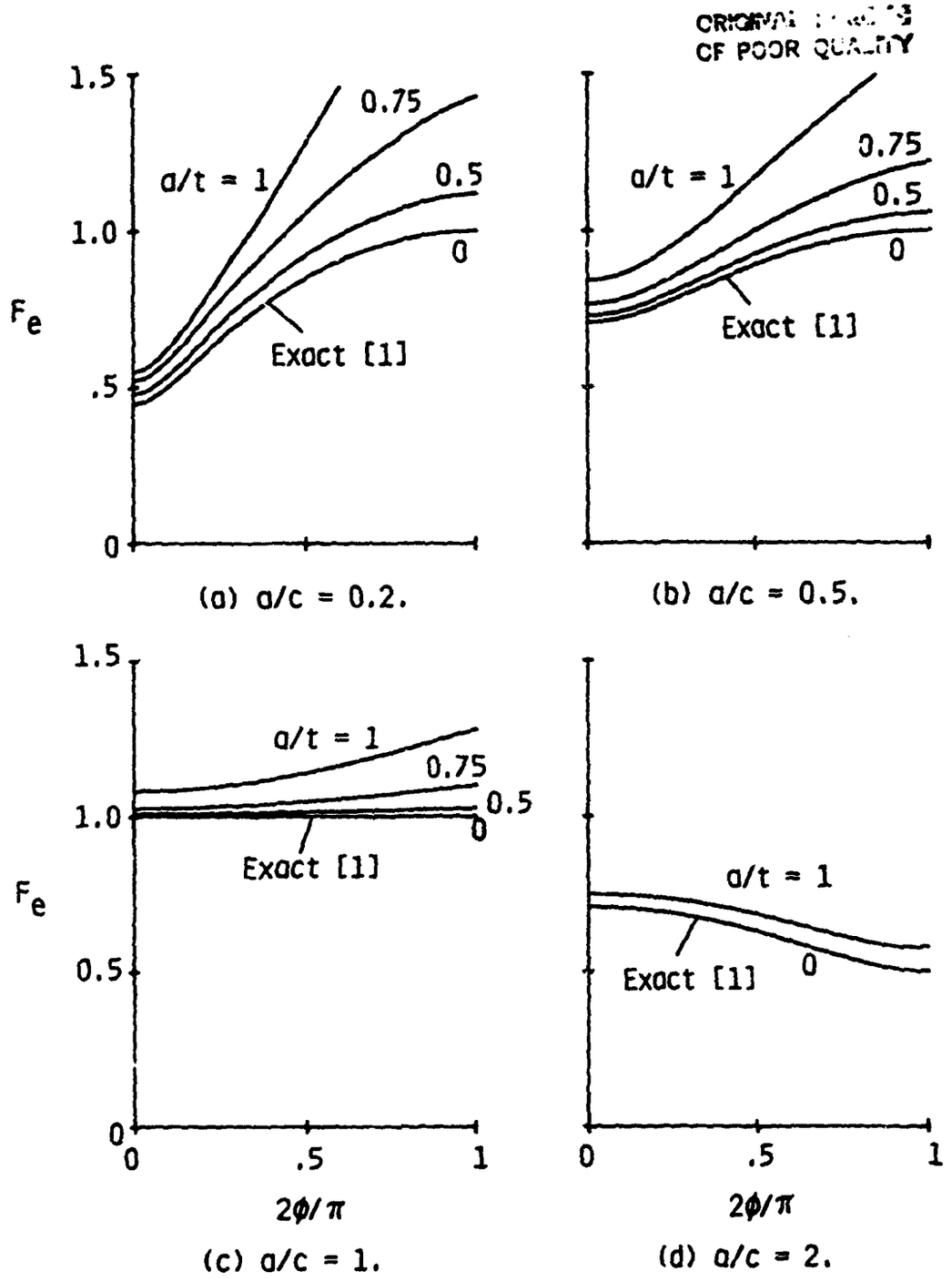

Fig. 4--Typical boundary-correction factors for an embedded elliptical crack in the center of a plate subjected to remote tension (c/b = 0).

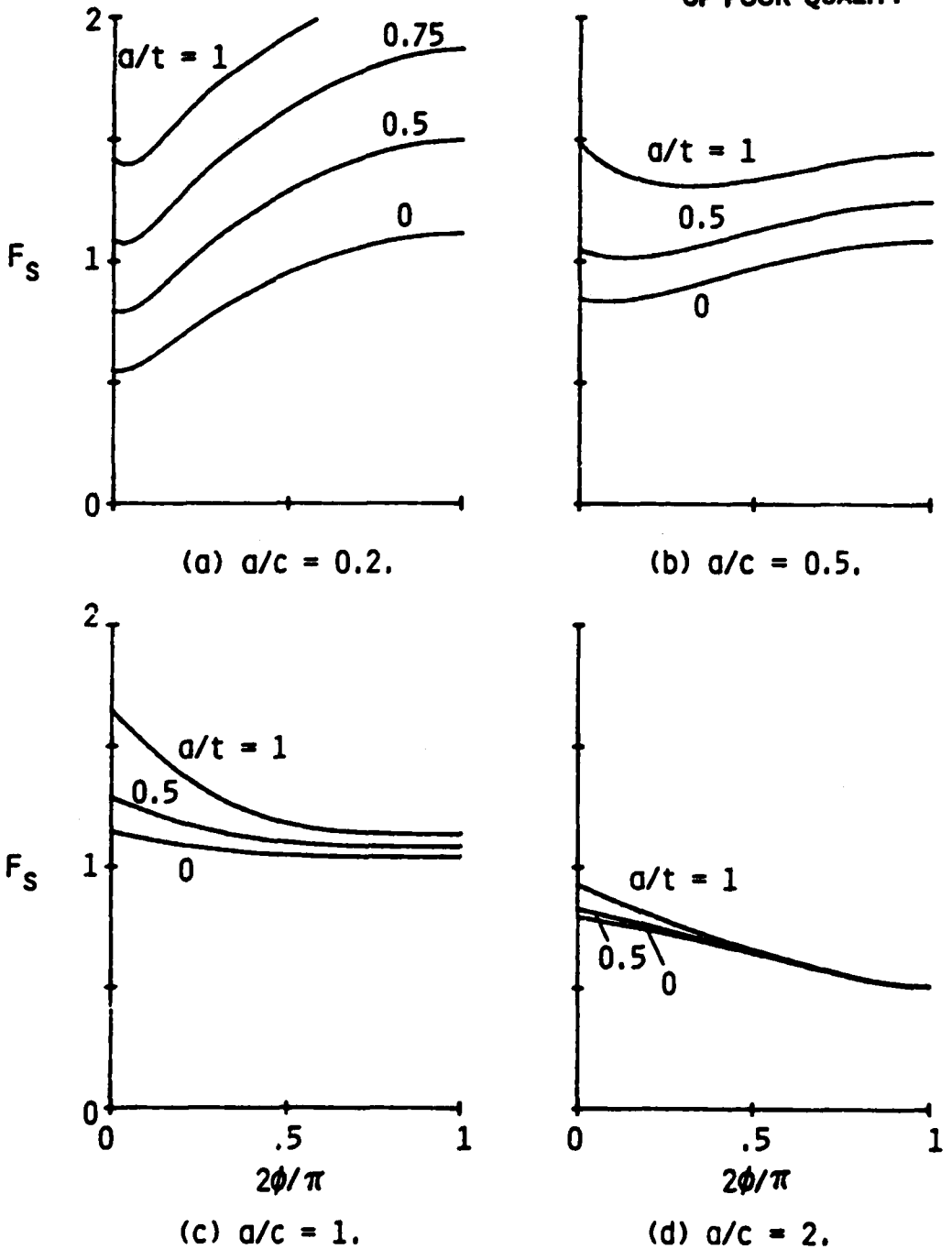

Fig. 5--Typical boundary-correction factors for a surface crack in a plate subjected to remote tension (c/b = 0).

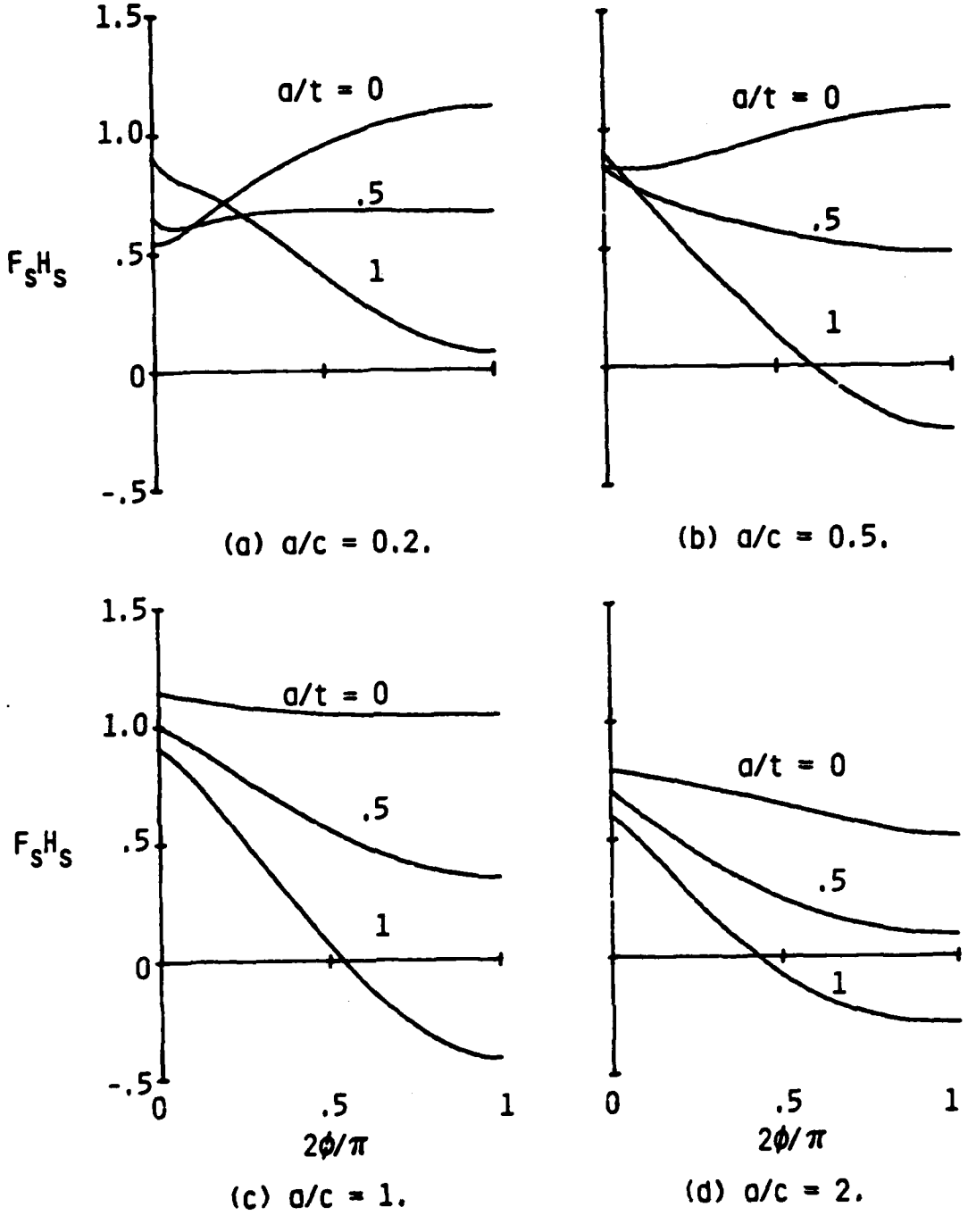

Fig. 6--Typical boundary-correction factors for a surface crack in a plate subjected to remote bending (c/b = 0).

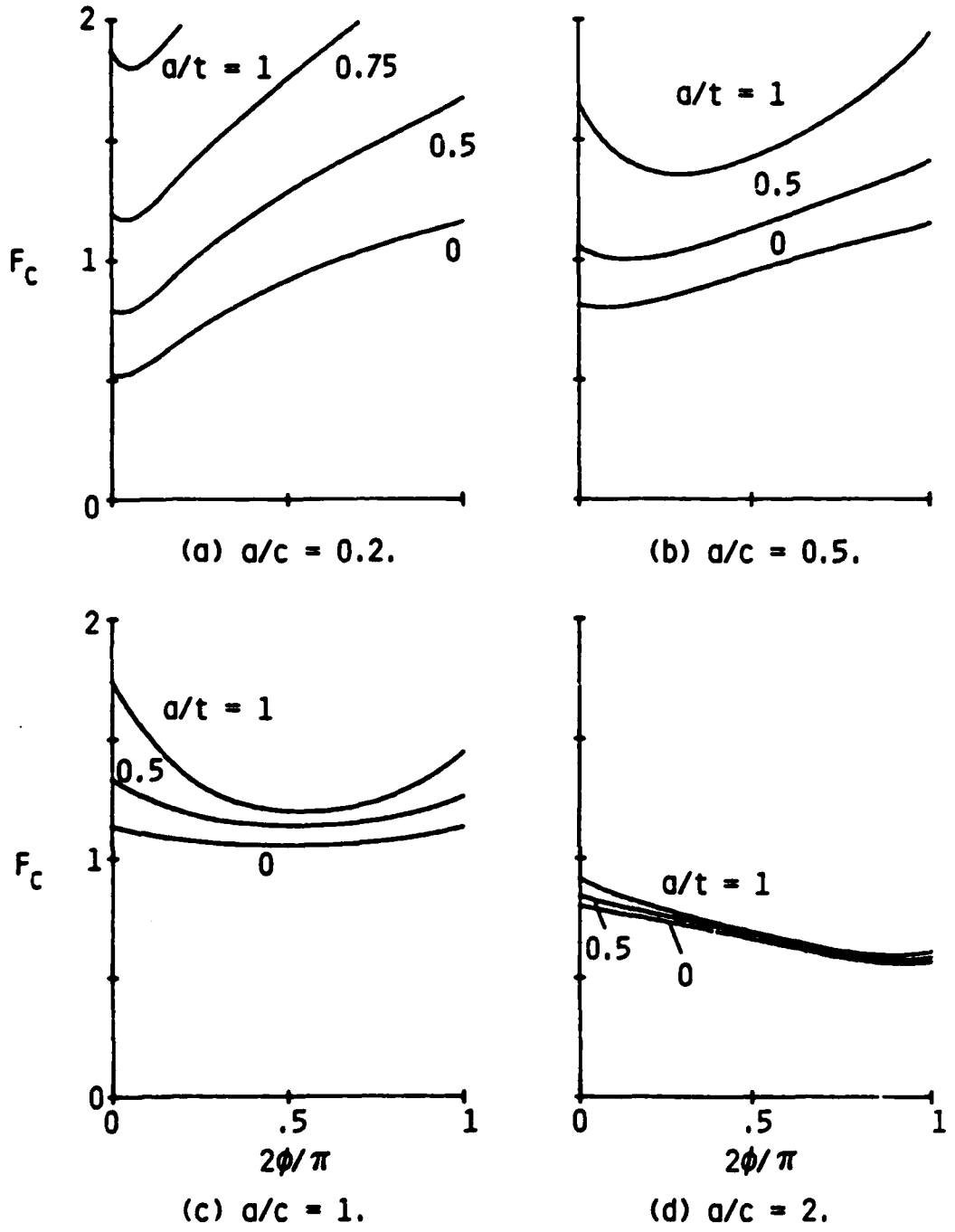

Fig. 7--Typical boundary-correction factors for a corner crack in a plate subjected to remote tension (c/b = 0).

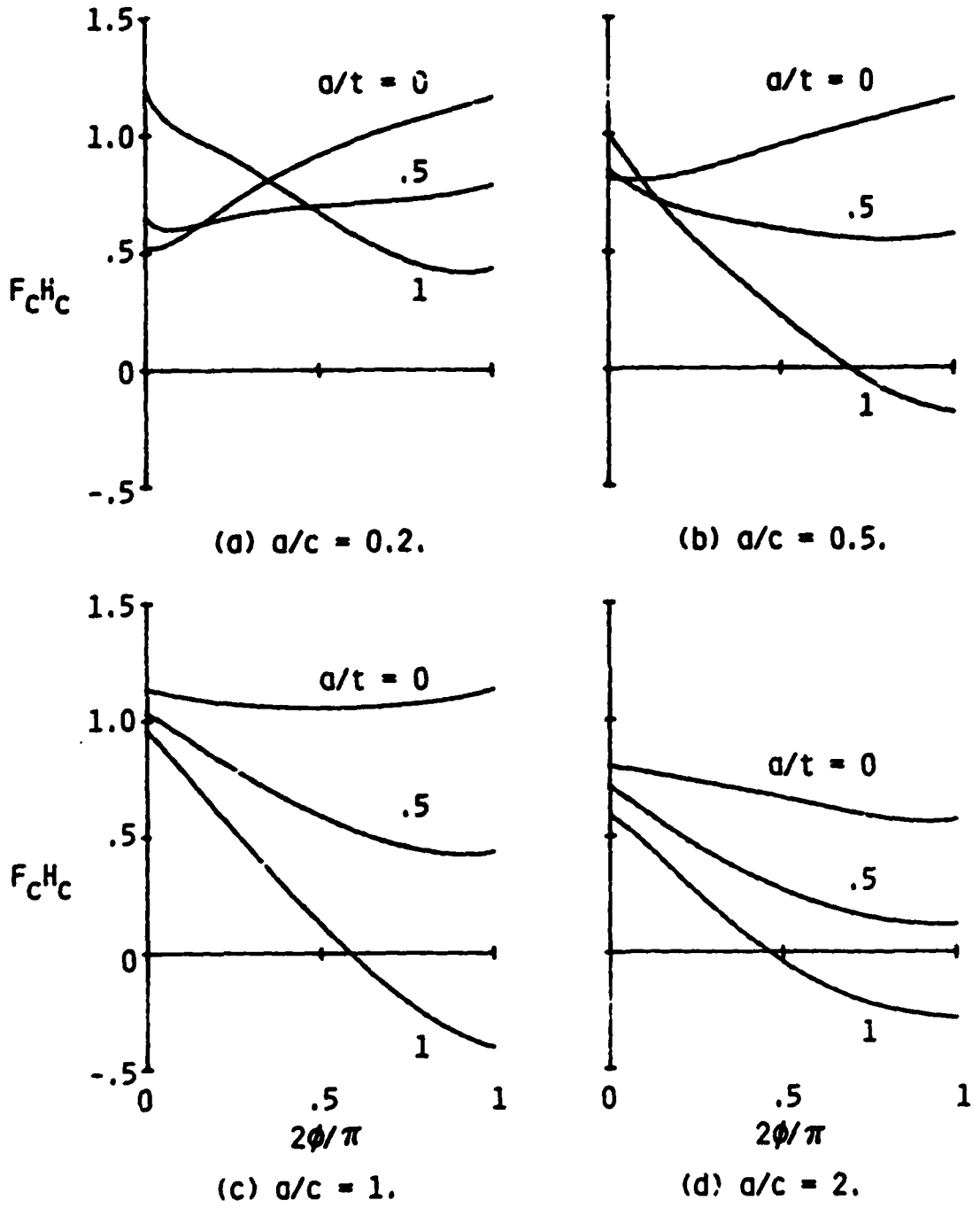

Fig. 8--Typical boundary-correction factors for a corner crack in a plate subjected to remote bending (c/b = 0).

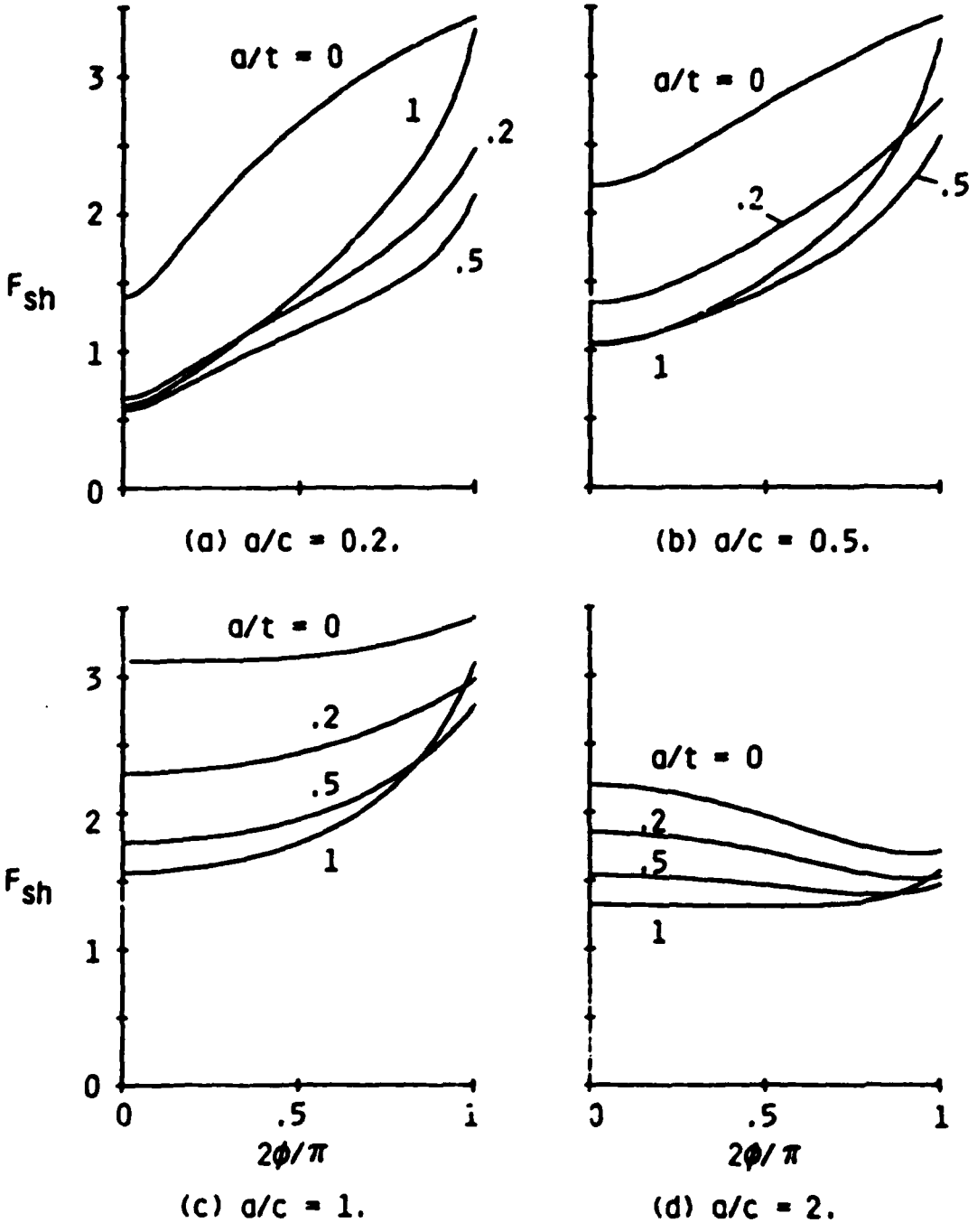

Fig. 9--Typical boundary correction factors for a single surface crack at the center of a circular hole in a plate subjected to remote tension (r/t = 1; r/b = 0).

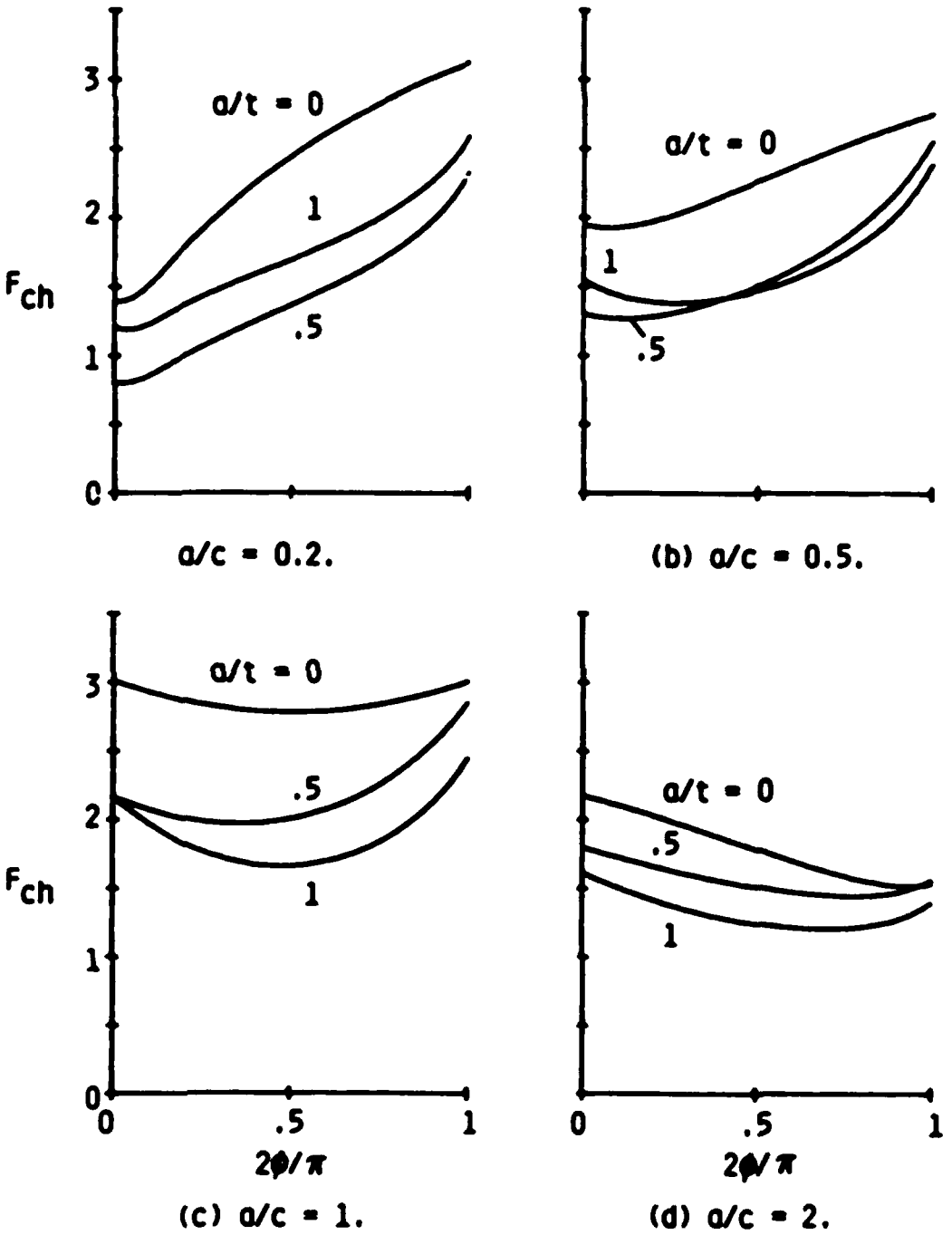

Fig. 10--Typical boundary-correction factors for a single corner crack at the edge of a circular hole in a plate subjected to remote tension (r/t = 1; r/b = 0).

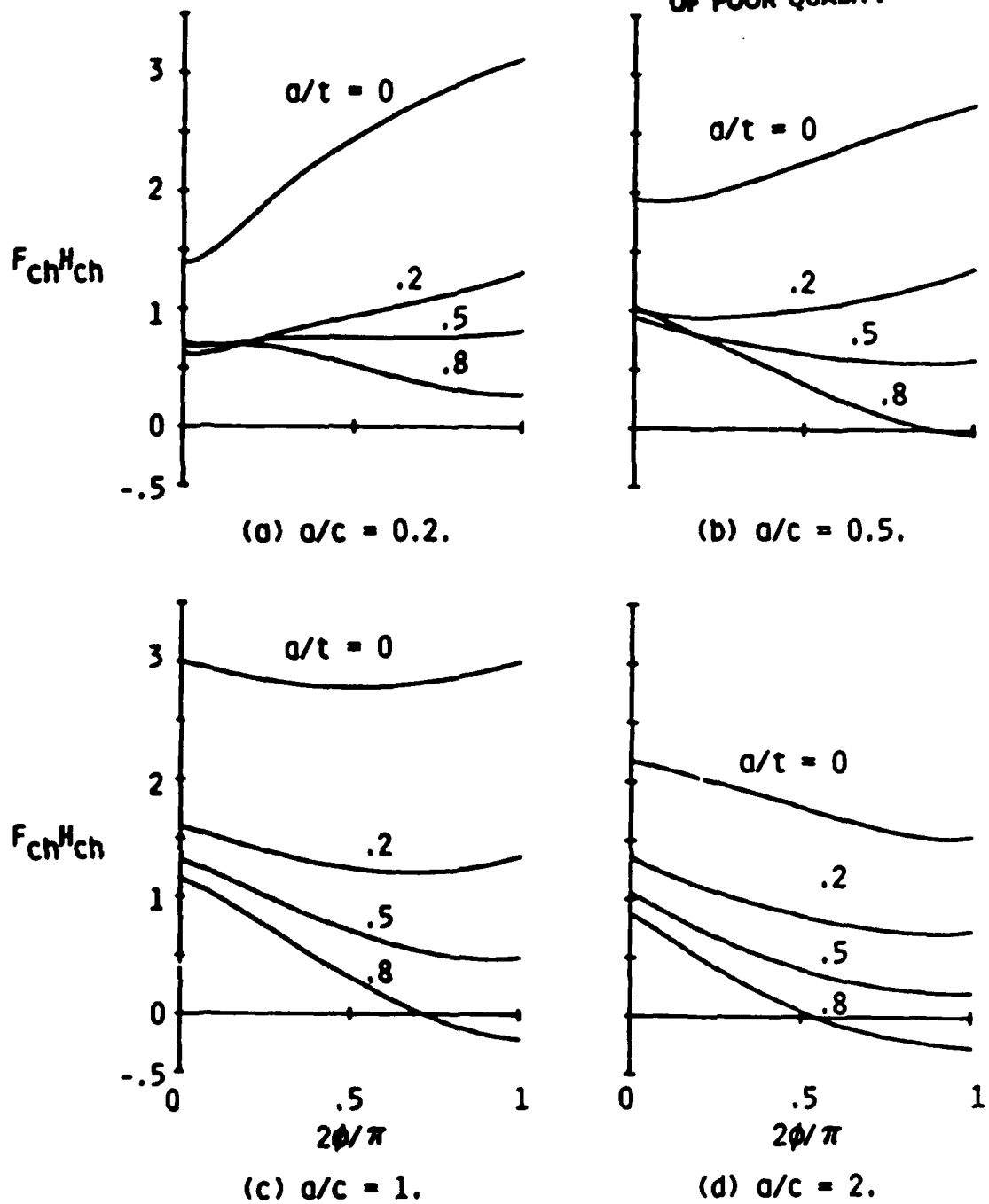

Fig. 11--Typical boundary-correction factors for a two-symmetric corner crack at the edge of a circular hole in a plate subjected to remote bending (r/t = 0.5; r/b = 0).